ELSEVIER

Original article

New cranial material of *Shansirhinus* (Rhinocerotidae, Perissodactyla) from the Lower Pliocene of the Linxia Basin in Gansu, China

Nouveau matériel crânien de *Shansirhinus* (Rhinocerotidae, Perissodactyla) de Pliocène inférieur du bassin de Linxia (Gansu, Chine)

Tao Deng

Institute of Vertebrate Paleontology and Paleoanthropology, Chinese Academy of Sciences, PO Box 643, Beijing 100044, China

Abstract

A well-preserved skull and articulated mandible of *Shansirhinus*, a horned aceratherine rhinocerotid, is described from an Early Pliocene (Gaozhuangian; approximately 5.3–4.34 Ma) locality of the Linxia Basin in Gansu, China. Comparing the new material of *Shansirhinus ringstromi* Kretzoi, 1942, we confirm the synonymy proposed previously for the species *Chilotherium yunnanensis* Tang et al., 1974, *Chilotherium cornutum* Qiu and Yan, 1982, and *Ch. tianzhuensis* Zheng, 1982. New knowledge concerning its cranial and mandibular morphology allows insight into its phylogenetic position among aceratherine rhinocerotids. A sister group relationship between *Shansirhinus* and *Chilotherium* is proposed on the basis of cranial, mandibular and dental evidence. Shared derived characters that support this relationship include: an expanded mandibular symphysis with a concave ventral surface; retracted premaxillae lacking upper incisors; a robust and right-angled facial crest; a flat or slightly concave dorsal skull profile; a weak or absent parastyle fold; and a constricted protocone on the premolars. *Shansirhinus* was probably a grazer, which is evidenced by the high crown, strong wear, well-developed secondary folds, and enamel plications on its teeth. The age of *S. ringstromi* is Late Miocene to the Early Pliocene, corresponding to the Turolian to Ruscinian, MN12–MN15 of Europe. *S. ringstromi* is likely the ancestor of the more advanced *S. brancoi* (Schlosser, 1903).

© 2005 Elsevier SAS. All rights reserved.

Résumé

Cet article décrit un crâne avec sa mandibule de *Shansirhinus ringstromi* Kretzoi, 1942 dont l'holotype, conservé à Uppsala, est un maxillaire avec ses rangées dentaires ; il provient de Huangshigou à Yushe (Shanxi). Le nouveau matériel autorise d'intéressantes conclusions systématiques, anatomiques et phylogénétiques. *Chilotherium yunnanensis* Tang et al., 1974, *Chilotherium cornutum* Qiu et Yan, 1982 et *Ch. tianzhuensis* Zheng, 1982 sont des synonymes récents de *S. ringstromi*. L'espèce présente de MN 12 à MN 15 est aussi connue des provinces de Gansu et de Yunnan. Elle se caractérise par son crâne à profil dorsal faiblement concave, sa face occipitale faiblement inclinée vers l'arrière et le bas, un intermaxillaire petit et dépourvu d'incisives supérieures, un nasal pointu, court et relevé, portant une corne. Les jugales supérieures sont hypsodontes avec un émail plissé à proximité du crochet et de la crista. Les prémolaires sont munies d'un pont entre protocône et hypocône, à médifossette fermée, à parastyle faible ou absent, avec constriction du protocône et à cingulum lingual continu ; la DP^1, très petite, est permanente. Le genre pourrait être un groupe-frère de *Chilotherium*, et *S. ringstromi* pourrait être l'ancêtre de *S. brancoi* (Schlosser, 1903).

© 2005 Elsevier SAS. All rights reserved.

E-mail address: dengtao@ivpp.ac.cn (T. Deng).

1. Introduction

The rhinoceroses of the Linxia Basin in Gansu, China have been studied by Qiu et al. (1987b, 1990, 2002); Qiu and Xie (1998); Guan (1988); Guan and Zhang (1993); Deng (2001b, 2001c, 2002a, 2002b, 2003). In 1998, many new well-preserved mammal fossils were collected from the red clay at Yinchuan in the Linxia Basin (Fig. 1). A complete rhinocerotid skull and articulated mandible is included in the collection from this locality, along with skulls of *Hipparion licenti* and *Gazella blacki*. The rhinocerotid material is the focus of this study.

The Yinchuan fossils are from the upper part of the Early Pliocene Hewangjia Formation (Fig. 2). The brown–red clay of the Liushu Formation underlies this section and has a thickness of 60 m. The Hewangjia Formation consists primarily of a 30-m-thick light red clay and a 5-m-thick basal conglomerate that is poorly rounded and sorted. The Jishi Conglomerate, which overlies the Hewangjia Formation, is 10 m in thickness, is well rounded and poorly sorted, and its largest gravel diameter is 30 cm. The Wucheng Loess overlies the Jishi Comglomerate, and this brownish yellow loess is banded by brownish red paleosol.

Terminology and taxonomy follow Heissig (1972, 1999); Guérin (1980). The measurements are according to Guérin (1980) and are given in mm. The studied material is housed at the Institute of Vertebrate Paleontology and Paleoanthropology in Beijing. Abbreviations: IVPP or V, Institute of Vertebrate Paleontology and Paleoanthropology, Chinese Academy of Sciences, Beijing, China. M, Evolution Museum, University of Uppsala, Uppsala, Sweden. L, length; W, width; H, height.
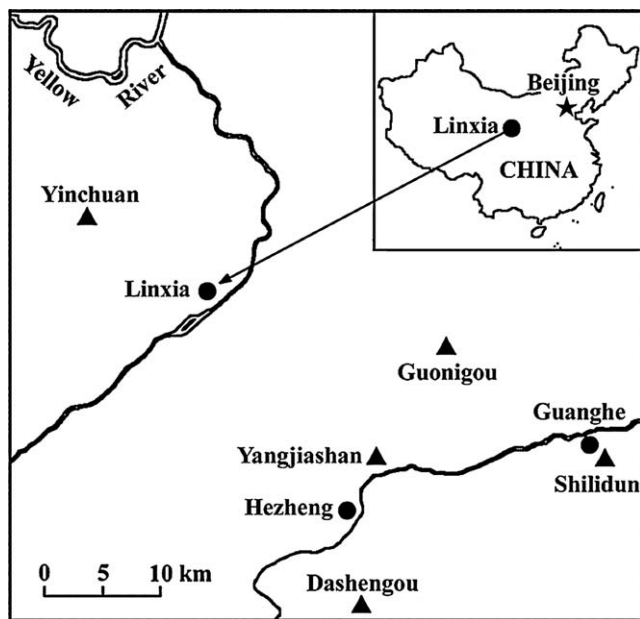

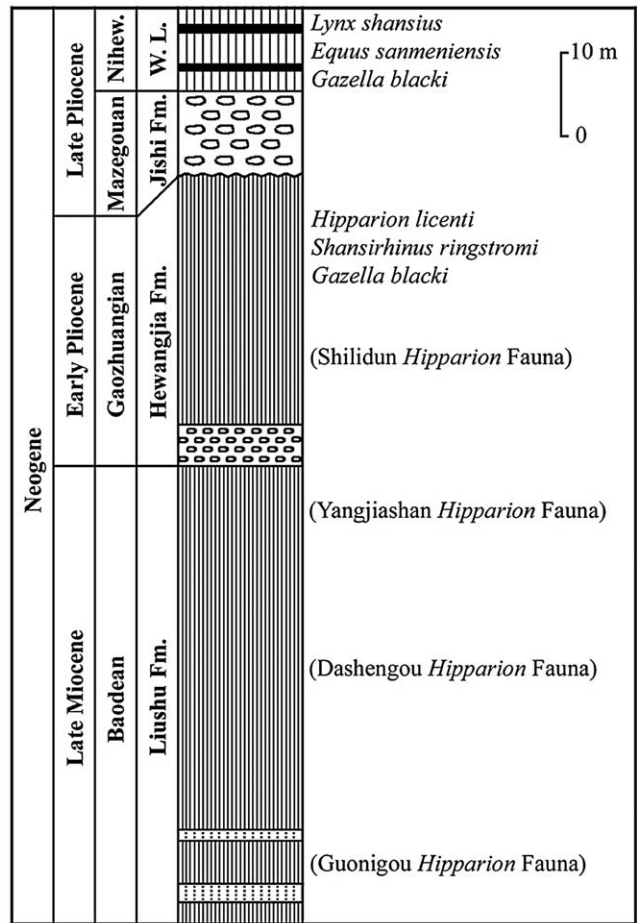Fig. 1. Location map.
Fig. 1. Carte de localisation.

Fig. 2. Generalized stratigraphic section.
Fig. 2. Colonne stratigraphique généralisée.

2. Systematic paleontology

Order PERISSODACTYLA Owen, 1848.
Family RHINOCEROTIDAE Gill, 1872.
Subfamily ACERATHERIINAE Dollo, 1885.
Tribe CHILOTHERIINI Qiu et al., 1987b.
Genus **Shansirhinus** Kretzoi, 1942.
Shansirhinus ringstromi Kretzoi, 1942.
Figs. 3–6 and Tables 1–4.
Synonymy:
1927. *R.* aff. *brancoi*—Ringström, pp. 15–18, Pl. 1, Fig. 3.
1974. *Chilotherium yunnanensis* sp. nov.—Tang et al., pp. 63–65, Pl. 1, Fig. 3.
1982. *Chilotherium cornutum* sp. nov.—Qiu and Yan, pp. 122–132, Text-Figs. 1–7, Pls. 1, 2.
1982. *Chilotherium tianzhuensis* sp. nov.—Zheng, pp. 219–221, Pl. 1, Figs. 5 and 6, Pl. 2, Fig. 1.
1987b. *Acerorhinus cornutus*–Qiu et al., pp. 549–551.
Lectotype: M 536, a maxillary with complete cheek tooth rows from Huangshigou (Huang-Shih-Kou) in Yushe (Shanxi, China) (Ringström, 1927: Pl. 1, Fig. 3). Stored in the Evolution Museum, University of Uppsala (Uppsala, Sweden).
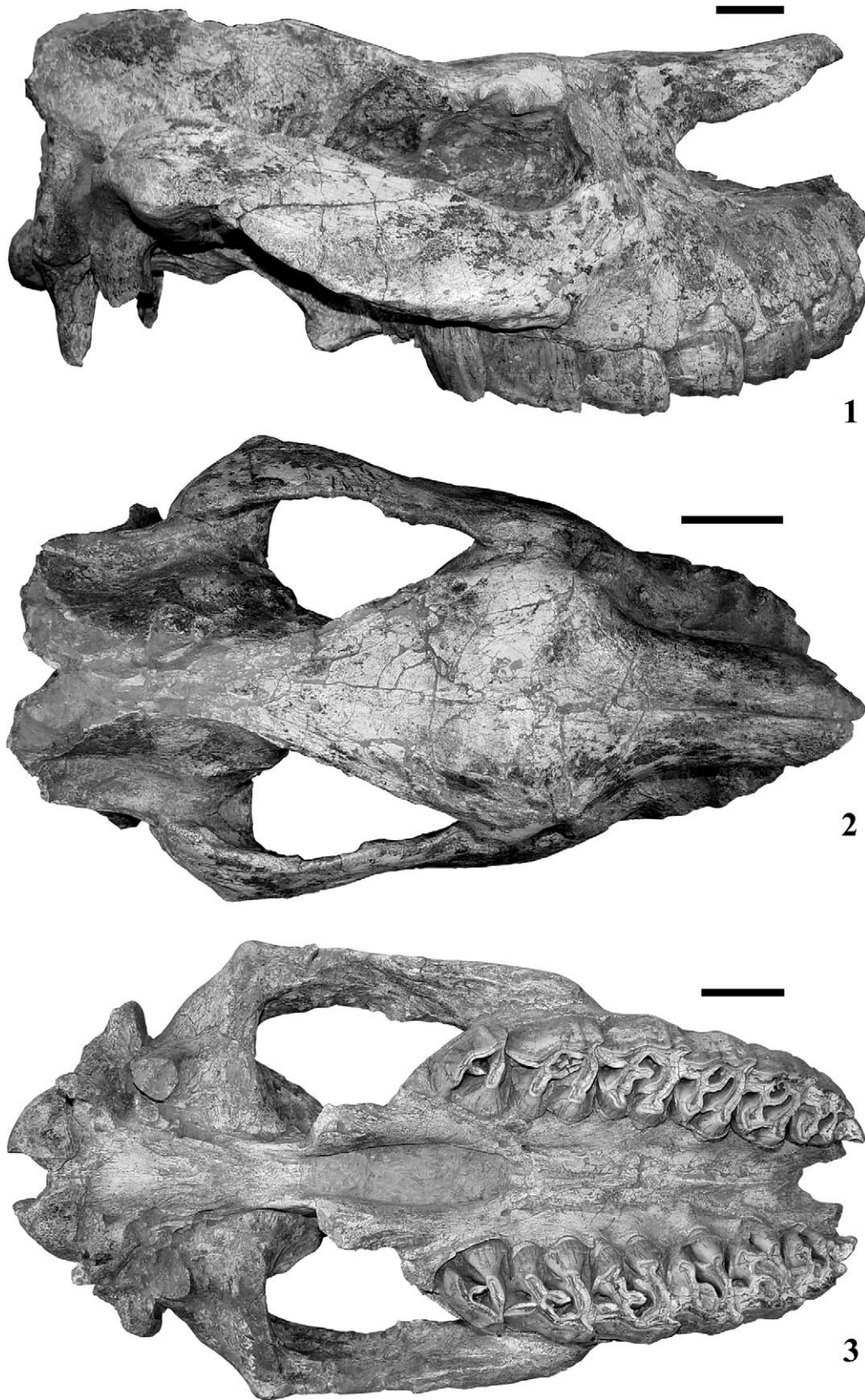**Geographical distribution**: Shanxi, Gansu, and Yunnan Provinces in China.

Fig. 3. Mandible of *S. ringstromi* from Yinchuan, Linxia (Gansu, China), V 13764, scale bar = 5 cm. (**1**) Lateral view. (**2**) Occlusal view.
Fig. 3. Mandibule de *S. ringstromi* de Yinchuan, Linxia (Gansu, Chine), V 13764, barre d'échelle = 5 cm. (**1**) Vue latérale. (**2**) Vue occlusale.
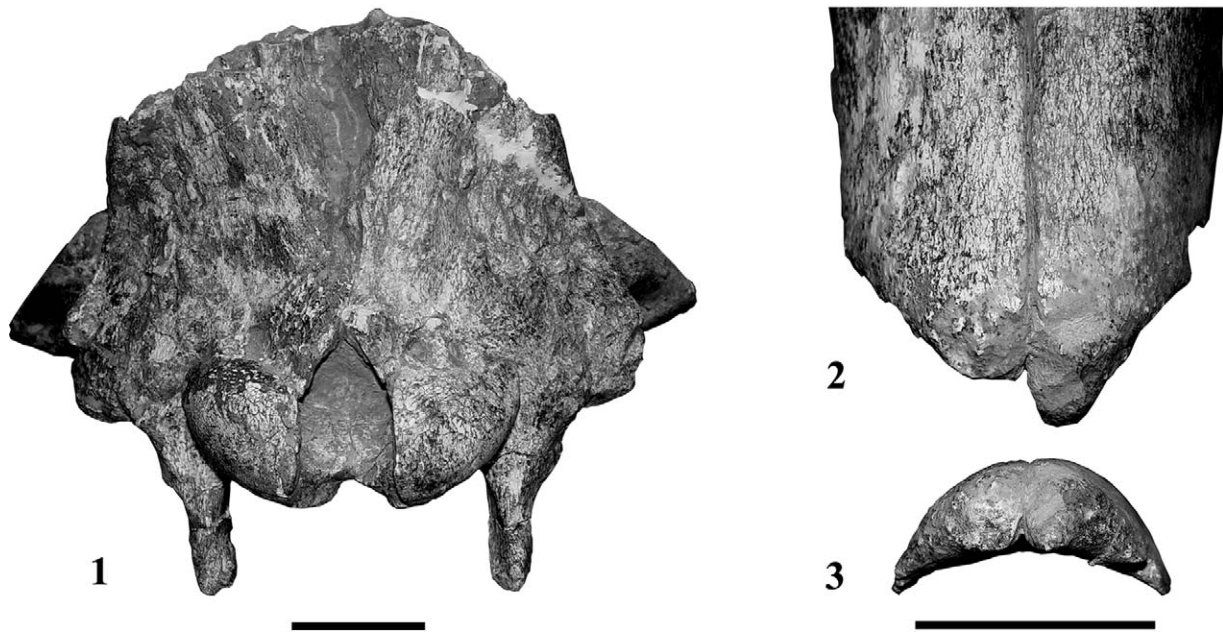
Fig. 4. Skull of *S. ringstromi* from Yinchuan, Linxia (Gansu, China), V 13764, scale bar = 5 cm. (**1**) Lateral view. (**2**) Dorsal view. (**3**) Occlusal view.
Fig. 4. Crâne de *S. ringstromi* de Yinchuan, Linxia (Gansu, Chine), V 13764, barre d'échelle = 5 cm. (**1**) Vue latérale. (**2**) Vue supérieure. (**3**) Vue occlusale.

Table 1
Measurements and comparisons of skull of *S. ringstromi* (V 13764) from Yinchuan, Linxia (Gansu, China) in millimeters
Mesures et comparaisons en millimètres du crâne de *S. ringstromi* (V 13764) de Yinchuan, Linxia (Gansu, Chine)

| Measures	*S. ringstromi* (Yinchuan)	*Ch. Cornutum* (Qiu and Yan, 1982)
1 Distance between occipital condyle and premaxillary tip	>520	
2 Distance between occipital condyle and nasal tip	515	
3 Distance between nasal tip and occipital crest	~480	
4 Distance between nasal tip and bottom of nasal notch	118	114
5 Minimal width of braincase	75	
6 Distance between occipital crest and postorbital process	~280	
7 Distance between occipital crest and supraorbital tubercle	~295	
8 Distance between occipital crest and lacrimal tubercle	~340	
9 Distance between nasal notch and orbit	63	60
13 Distance between occipital condyle and M^3	264	
14 Distance between nasal tip and orbit	176	
15 Width of occipital crest	~155	
16 Width between mastoid processes	211	
17 Minimal width between parietal crests	~40	
18 Width between postorbital processes	155	
19 Width between supraorbital tubercles	174	175
20 Width between lacrimal tubercles	168	
21 Maximal width between zygomatic arches	295	
22 Width of nasal base	84	75
23 Height of occipital surface	~125	
25 Cranial height in front of P^2	146	
26 Cranial height in front of M^1	180	
27 Cranial height in front of M^3	170	
28 Palatal width in front of P^2	52	
29 Palatal width in front of M^1	73	
30 Palatal width in front of M^3	70	
31 Width of foramen magnum	37.5	
32 Width between exterior borders of occipital condyles	113	
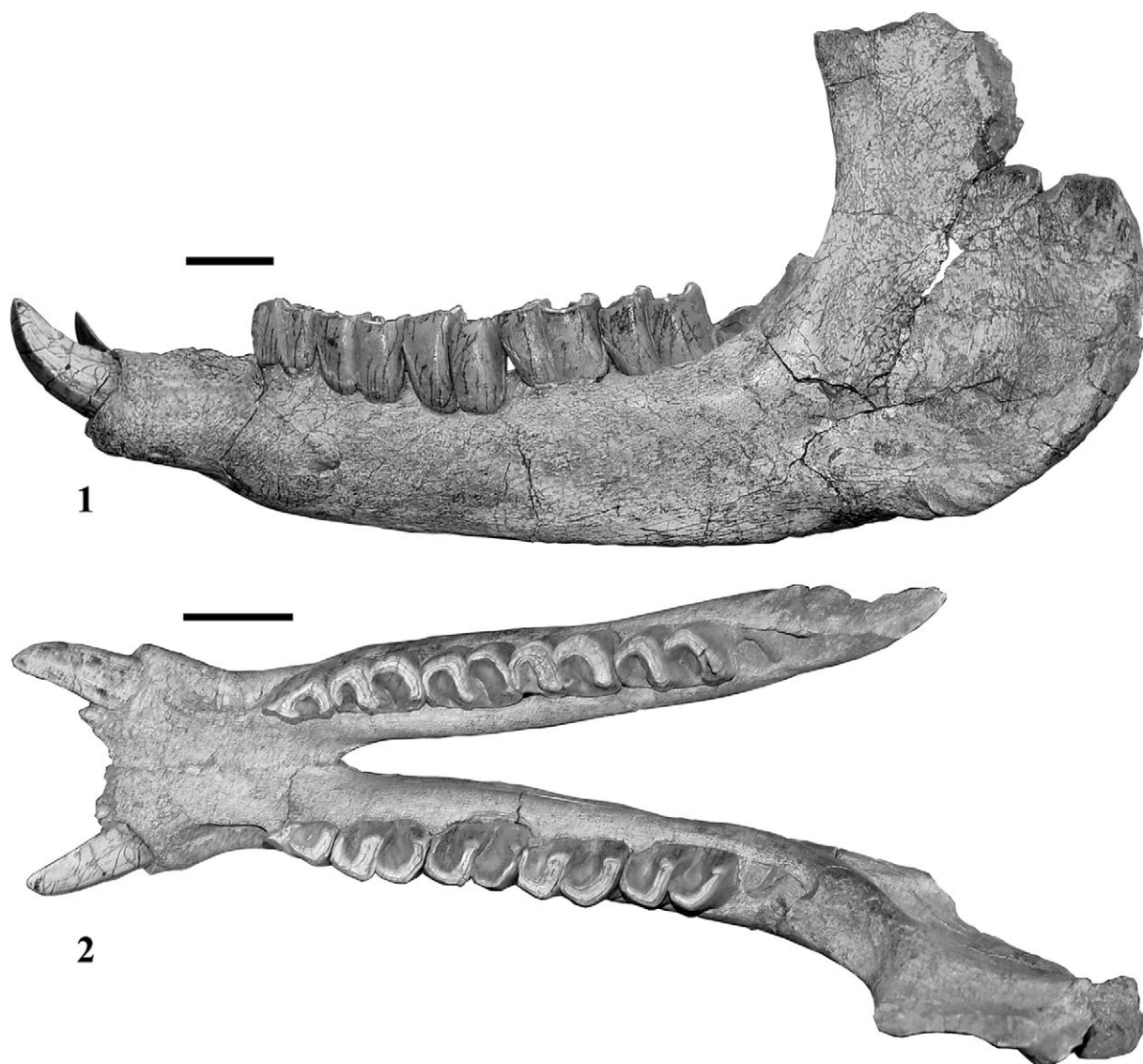
Fig. 5. Occipital surface and nasals of *S. ringstromi* from Yinchuan, Linxia (Gansu, China), V 13764, scale bar = 5 cm. (**1**) Occipital surface. (**2**) Nasals in dorsal view. (**3**) Nasals in anterior view.

Fig. 5. Face occipitale et nasale de *S. ringstromi* de Yinchuan, Linxia (Gansu, Chine), V 13764, barre d'échelle = 5 cm. (**1**) Face occipitale. (**2**) Nasale en vue supérieure. (**3**) Nasale en vue antérieure.

Table 2
Measurements of mandible of *S. ringstromi* (V 13764) from Yinchuan, Linxia (Gansu, China) in millimeters
Mesures en millimètres de la mandibule de *S. ringstromi* (V 13764) de Yinchuan, Linxia (Gansu, Chine)

Measures	V 13764
1 Length	460
2 Distance between posterior borders of symphysis and ascending ramus	360
3 Height of horizontal ramus in front of P_3	63
4 Height of horizontal ramus in front of P_4	67
5 Height of horizontal ramus in front of M_1	70
6 Height of horizontal ramus in front of M_2	77
7 Height of horizontal ramus in front of M_3	83
9 Distance between horizontal rami in front of M_1	65
10 Distance between horizontal rami in front of M_3	77
11 Length of symphysis	104
13 Antero-posterior diameter of ascending ramus	134.5

Fig. 6. Teeth of *S. ringstromi* from Yinchuan, Linxia (Gansu, China), V 13764, occlusal view, scale bar = 5 cm. (**1**) Right upper tooth row. (**2**). Right lower tooth row.

Fig. 6. Dents de *S. ringstromi* de Yinchuan, Linxia (Gansu, Chine), V 13764, vue occlusale, barre d'échelle = 5 cm. (**1**) Série dentaire supérieure droite. (**2**) Série dentaire inférieure droite.

Table 3

Measurements and comparisons of upper teeth of *S. ringstromi* (V 13764) from Yinchuan, Linxia (Gansu, China) in millimeters

Mesures et comparaisons en millimètres des dents supérieures de *S. ringstromi* (V 13764) de Yinchuan, Linxia (Gansu, Chine)

	Upper teeth	*S. ringstromi* (Yinchuan)	*R.* aff. *brancoi* (Ringström, 1927)	*Ch. yunnanensis* (Tang et al., 1974)	*Ch. cornutum* (Qiu and Yan, 1982)	*Ch. tianzhuensis* (Zheng, 1982)	*R. brancoi* (Schlosser, 1903)
DP¹	L	21.5	19		18	17.7	
	W	20	20.5		17	17.2	
	H	21	16				
P²	L	38	42.5	>34	38	34.9	
	W	45	51.5	38	44	42.4	
	H	36	40	23			
P³	L	43.5	44.5	38	42	36.9	30?
	W	57	60	>48	54	50.8	35
	H	36	46	33			32?
P⁴	L	43	45.5	>38	43	41.1	42
	W	63	65	>52	59	56.5	54
	H	43	52	34			50
M¹	L	52	52	>41	50	48.1	47
	W	62	70	>53	60	58.1	48
	H	44	50	30			51
M²	L	53.5	55		57	51.1	
	W	61.5	67.5		61	56.1	
	H	48	55				
M³	L	52			50	40.4	
	W	55			57	49.7	
	H	51					

Table 4

Measurements of lower teeth of *S. ringstromi* (V 13764) from Yinchuan, Linxia (Gansu, China) in millimeters

Mesures et comparaisons en millimètres des dents inférieures de *S. ringstromi* (V 13764) de Yinchuan, Linxia (Gansu, Chine)

Lower teeth		*S. ringstromi* (Yinchuan)	*R. brancoi* (Schlosser, 1903)
P_2	L	31	
	W	20.5	
	H	32	
P_3	L	39	
	W	26.5	
	H	34	
P_4	L	39	33
	W	30	24
	H	43	37.5
M_1	L	42.5	35
	W	29.5	25
	H	33	39
M_2	L	41.5	38
	W	27	25
	H	34	45

Stratigraphical distribution: Upper Miocene to Lower Pliocene, Upper Baodean to Gaozhuangian of China, corresponding to the Turolian to Ruscinian, MN12–MN15 of Europe.

Diagnosis: The premaxillae are significantly retracted and lack upper incisors. The nasals are short and raised, with a rough horn boss on the tip. The mandibular symphysis is moderately expanded, with a concave labial surface. DP^1 is very small. The protocone is strongly constricted. The bridge and medifossette are well-developed on the premolars, with elaborate enamel plications and a continuous lingual cingulum present. The trigonid is angularly U-shaped.

Material studied: IVPP V 13764, a complete skull and articulated mandible from the Gaozhuangian of the Lower Pliocene (MN15) at Yinchuan in the Linxia Basin (Gansu, China).

Description: The Yinchuan skull (V 13764) is relatively complete and only somewhat broken on the premaxillae, postglenoid processes and occipital crest. The mandible is missing the right ascending ramus and the upper part of the left ascending ramus. This is a sub-adult individual with a lightly worn M^3, a barely erupted M_3, and a weak dI_1. All of the teeth are relatively unworn, but many of the sutures have been fused, making recognition of some individual bones difficult.

Skull—The skull is short, with a length of 515 mm from the nasal tip to the occipital condyle. The nasals are wide and short, with a width of 84 mm at the nasal base and a length of 118 mm from the nasal tip to the bottom of the nasal notch. The nasals have a convex and smooth dorsal surface, with a weak lateral process on the lower margin. The nasal central suture is not completely fused, having separate tips and a narrow groove on the posterior end. The left tip is sharp but the right tip is rounded, and both are rough, indicating the presence of a small horn boss (Qiu and Yan, 1982). The nasals are

slightly uplifted and have a weakly declined tip, and the nasal base is slightly constricted. The dorsal transverse profile of the nasals is M-shaped and the ventral surface is flat. There are three small and sharp infraorbital foramina at the level of the P^3/P^4 boundary. Two are located near the bottom of the nasal notch on the maxillary face, with the anterior and lower one being larger and having a front groove. The smallest is located on the upper margin of the maxillary bone.

The nasal notch is narrow and angularly U-shaped at the level of the anterior part of P^4, with a height of 49 mm at its mid-section from the upper margin of the maxillary bone to the nasal margin. The premaxillae are retracted and form two narrow flakes with a curvature toward the anterior margin of the maxillary. The maxillary is convex, but has a wide depression anterior to the orbit. The position of the orbit is low, with a distance of 29 mm between its upper margin and the skull roof. The entire orbit is not prominent, but its anterior margin projects at the level of the posterior part of M^1. The supraorbital tubercle is robust and sharp, the lacrimal tubercle is miniscule at the mid-anterior margin of the orbit, and the frontal postorbital process is weak. The zygomatic arch is positioned low and has a weak postorbital process. The anterior end of the zygomatic arch is located at the level of the M^1/M^2 boundary, and it narrows slightly and connects with the facial crest. The facial crest is massive and forms an approximate right angel. The lower margin of the zygomatic arch is curved, and its anterior region approaches the alveolar border. The posterior region of the zygomatic arch is slightly expanded and strongly declined laterally, with a width of 54.5 mm at the level in front of the temporal condyle, and has a forwardly oblique posterior margin.

In lateral view, the dorsal skull profile is slightly concave. The skull roof is rhombic and is the widest between the supraorbital tubercles, with a weak depression on the frontal. The braincase is moderately wide, with a smallest width of 75 mm. The parietal crests are strong and consist of many small tubercles. The parietal crests have a flat surface between the anterior regions and narrow posteriorly, with a smallest width of about 40 mm. The occipital surface is slightly reclined posteriorly, with robust and convex lateral crests, but lack the nuchal tubercle and median and exterior crests. The lateral margins of the occipital crest are forwardly oblique and slightly divergent. The foramen magnum is narrow, highly positioned, and triangular. Its upper border is positioned much higher than that of the occipital condyle, with a distance of 21 mm between them. The nuchal ligament depression is a narrow, deep and highly inverse triangle. The postglenoid process is strong, and the paroccipital process is a long, tapering rod with three edges. The posttympanic process is 24.4 mm thick, has a rough margin, and joins the paroccipital process at the base. The posttympanic process fuses with the postglenoid process at the midpoint of the latter to form a pseudoauditory meatus. The temporal crest above the meatus is flat and has a high and thin crimping margin. The basilar tubercle is highly prominent, with a sagittal and several transverse crests. The basioccipital is positioned at an angle of about

$12°$ relative to the basisphenoid, and is posteriorly wide, convex, and triangular. The intercondyloid notch is wide and shallow, and has a width of 16.5 mm.

The palate has a sharp central crest, its posterior margin is narrowly U-shaped at the level of the M^2/M^3 boundary, and it has a small but prominent tubercle on its bottom. The palate is widely and strongly arched and has a width of 73 mm at the level of the P^4/M^1 boundary. The bottom of the palatine fissure is located at the level of the posterior part of dP^1, and the anterior palatine foramen is at the level of the hypocone of M^2. The maxillary tubercle is well developed.

The pterygoid bones have a vertical posterior margin and a narrow and deep valley between them. The vomer extends a length of 40 mm to the palate surface. The anterior border of the temporal fossa is located at the level of the anterior part of the M^3. The temporal condyle is convex, and the glenoid cavity is smooth laterally and has a wide crest medially. In ventral view, the anterior part of the zygomatic arch is thick and rough and has a laterally prominent anterior end, while the posterior region is thin and smooth.

Upper teeth—Because the premaxillae are strongly retracted, the upper incisors are absent. Both cheek tooth rows are forwardly convergent, and the length ratio of premolars to molars is 97% (134/138 mm), respectively, at the midline of the occlusal surface. The enamel is not wrinkled like that of elasmotheres, but has rich plications. The labial wall of the cheek teeth is slightly undulated and is covered by irregular cement, with the exception of M^3, and has upwardly divergent fine lines on the exposed parts. The tooth crown is moderately high, and the lightly worn M^3 has a height of 51 mm. The labial cingulum is absent, and the parastyle is strong.

DP^1 is very small, with a width of 20 mm posteriorly; it is double-rooted, with an antero-lingual cingulum; and the crista is marked, but the protoloph and crochet are absent. The premolars from P^2 to P^4 have a weak parastyle fold, but this fold is appreciably more obvious on P^4; the lingual valley is angularly U-shaped and the lingual cingulum is continuous and strong, linking the anterior and posterior cingula; the crochet is well-developed and forms a strong medifossette with the crista, and the lingual margin is rounded. The protocone and hypocone of P^2 are separated on the occlusal surface, but are fused together toward the base; the antecrochet is weak, and the hypocone is squarely expanded; and the protoloph has a weak enamel plication on the anterior wall, and the metaloph is posteriorly oblique. A large pillar is present at the entrance of the median valley of P^3. The protocone on P^3 and P^4 is strongly constricted and connects with the hypocone by the lingual bridge; the antecrochet is well-developed and the hypocone is not constricted; the metaloph is forwardly oblique labially but backwardly oblique lingually; and the medifossette has two or three enamel plications.

On the molars, the crochet is strong, and the crista is absent; the antecrochet is well developed, and its end extends lingually but does not reach the entrance of the median valley; the lingual margin of the protocone is flat; the anterior cingulum is well developed, the lingual cingulum forms a weak

pillar at the entrance of the median valley, and the posterior cingulum is reduced, leaving the posterior valley open. M^1 and M^2 have a moderately constricted protocone, a long metastyle and metaloph, a moderate parastyle fold, and a weak metacone fold. The hypocone of M^1 is evidently constricted, while that of M^2 is constricted only toward the base. M^2 has 2 weak enamel plications on the interior wall of the ectoloph. M^3 is triangular and has a weak posterior groove; the protocone is not constricted on the occlusal surface, but is strongly constricted near the base; the crista is weak, and the antecrochet is present on the lower part of the crown; the protoloph is posteriorly oblique and the lingual cingulum forms weak pillars on the lingual margin of the protocone; the posterior cingulum is low and close to the alveolar border; and the parastyle fold is prominent the middle region of the crown.

Mandible—In lateral view, the symphysis is thick, and almost flatly extends forward, with an angular transition to the lower margin of the horizontal ramus. In dorsal view, the symphysis is a moderately wide shovel, with its anterior region laterally expended and a posterior border at the level of the P_2/P_3 boundary. The symphysis is widest at the lateral border of the alveolus of I_2 on the anterior margin, with a width of 106.5 mm. It is narrowest at the position 20 mm from the anterior margin of P_2 on its posterior, with a width of 83.5 mm. The diastema between I_2 and P_2 is 62 mm in length and the alveolar crest is high and sharp, with a small arched posterior end that reaches P_2 and a large arched anterior end that extends, but does not reach the labial margin of I_2. The dorsal surface of the symphysis has a wide and deep V-shaped sagittal valley, and the ventral surface has a wide and deep U-shaped depression. As a result, the symphysis is very thin along its central line. Two large nutrition foramina are symmetrically positioned on the ventral surface of the symphysis and each has a diameter of 9.5 mm. The diastema between the two I_2s is 51 mm in length and is intermediate in length to those of *Acerorhinus* and *Chilotherium*. A small peg-like dI_1 is present near the base of I_2, and the anterior margin of the symphysis between the two dI_1s is sharp and concave. The mental foramen is long and narrow, with a length of 18 mm and a width of 7 mm. It is located at the level of the trigonid of P_3 near the lower margin of the horizontal ramus and has an anterior entrance.

The horizontal ramus is thick, 45 mm at the level of the P_4/M_1 boundary, and is positioned lower relative to the premolars than it is to the molars, so that the alveolar border forms a marked step at the P_4/M_1 boundary; its lower margin is slightly curved, and the sagittal lingual groove is wide and shallow on its interior wall. The mandibular angle is rounded and smooth, with an obvious vasal notch, and its margin is strong and prominent, with a thickness of 33 mm.

The ascending ramus is inclined forward and has smooth anterior, exterior and interior surfaces; and the lower anterior surface is wide and the medial surface is concave, causing the central part of the ascending ramus to be thin. The mandibular fossa is somewhat fragmented, but it may be large and round. There is a strong tubercle at the medial junction between the horizontal and ascending rami.

Lower teeth—The I_2 is a small tusk (crown dimensions: 59 mm long, 33.5 mm wide, and 17.5 mm thick); it is strongly uplifted but slightly extended laterally, and its crown is appreciably curved backward; and its medial flange is evidently upturned, and its worn surface faces posteriorly and laterally. DI_2 is small and peg-like, lacks enamel, and has a diameter of 5 mm and a length of 10 mm.

DP_1 is absent. The length of the lower premolars is 111.5 mm at the middle of the occlusal surface. On the lower cheek teeth, the crown is relatively high, and the highest P_4 has a crown of 43 mm at a light abrasion; the labial groove is narrowly and deeply V-shaped down to the base; the trigonid is angularly U-shaped, with a narrow and long paralophid and a right-angled metalophid; and the metaconid is not constricted but has a weak anterior groove on M_1. On the lower premolars, the posterior valley is widely V-shaped lingually; the lingual and labial cingula are absent, but a weak and low pillar is present on the bottom of the labial groove of the P_2; and the vertical lines on the labial wall are weak. P_2 is double-rooted; the trigonid is reduced and extends forward, narrowly and sharply, and the ectolophid fold is sharp and reclines backward. On the lower molars, the lingual and labial cingula are absent, the hypolophid reclines backward, and the entoconid has a flat lingual margin.

3. Comparison

Schlosser (1903) described a new rhinocerotid species, *Rhinoceros brancoi*, based on some insolate teeth that were purchased from drug stores in China. The morphological characters of those teeth are very peculiar. On the premolars, rich enamel plications are developed around the crochet and crista, two or three medifossettes are present on each premolar, and a strong lingual bridge connects the protoloph with the metaloph. On the molars, the protocone is strongly constricted, the crochet and antecrochet are well developed, and the parastyle fold is weak on the labial wall. Ringström (1927) described a maxillary with complete cheek teeth from Huangshigou (Huang-Shih-Kou) in Yushe (Shanxi, China) as *R.* aff. *brancoi*, and its teeth are similar to those of Schlosser's specimens but have less enamel plications. Kretzoi (1942) considered the features of *R. brancoi* to be relatively distinct and suggested the establishment of a new genus, *Shansirhinus*. In addition to *S. brancoi*, he created another species, *S. ringstromi*, based on the maxillary of *R.* aff. *brancoi* that was described by Ringström (1927). The tooth crown of *S. ringstromi* is lower than that of *S. brancoi* and its enamel plications are much weaker than those of the latter. Heissig (1975) revised *R. brancoi* Schlosser into *Chilotherium brancoi* (Schlosser). However, the numerous enamel plications, the strongly bifurcate or trifurcate crochets, and the well-developed lingual bridges of *R. brancoi* are not characters of the genus *Chilotherium*.

The skull from Yinchuan resembles *S. ringstromi* Kretzoi from Huangshikou (Ringström, 1927: Pl. 1, Fig. 3) with respect to the maxillary and dental morphologies. Similarities include a narrow choana, a widely arched palate, and a relatively prominent anterior end of the zygomatic arch. The teeth are characterized by rich enamel plications, weak parastyle folds, a relatively small dP^1, very strong crochets, and strongly constricted protocones. The premolars have well-developed lingual bridges, strong medifossettes, angularly U-shaped lingual valleys, continuous lingual cingula, and squarely expanded hypocones. Differences also exist between the Yinchuan skull and the maxillary of *S. ringstromi* from Huangshikou. On the premolars of the latter, there are two or three medifossettes, the lingual bridges are strong, and the lingual pillar is absent on P^3. Because these differences represent individual variations within a species, we identify the Yinchuan skull as *S. ringstromi*.

The general dental characteristics of the Yinchuan skull are similar to those of *Shansirhinus brancoi* (Schlosser) from China (Schlosser, 1903: Pl. 5, Figs. 1–4, Pl. 6, Fig. 12) with respect to the rich enamel plications, the weak parastyle folds, the well-developed bridges on the upper premolars, and the right-angled U-shaped trigonids on the lower premolars. However, there are major differences between these two species. In the case of *S. brancoi*, the enamel plications are numerous and long, and the crochets are strongly bifurcate or trifurcate. Kretzoi (1942) suggested that the dental crown of *S. ringstromi* is lower than that of *S. brancoi*, but our data do not support his opinion (Table 3). The discovery of the Yinchuan skull permits a confident description of the cranial, mandibular and dental characters of *S. ringstromi*.

The Yinchuan skull differs from *Chilotherium* Ringström. In *Chilotherium*, the nasals are straight and long with a rounded and smooth tip, and the nasal base is not constricted; the nuchal tubercle on the occipital surface is strong, and the paroccipital process is slender; the mandibular symphysis is strongly expanded laterally and the ratio of its width to length is much larger than 1; the anterior margin of the symphysis between the two I_2s is straight, and the sagittal valley on the dorsal surface is shallow and U-shaped; the horizontal ramus is high, and the vasal notch is weak; the ascending ramus is vertical; the length of premolar is 70–80% of the molar length and dP^1 is comparatively large; the lingual cingulum is weak and discontinuous and the protocone is very strongly constricted; the lingual bridges are weak or absent, and the enamel plications are completely absent on the upper premolars; the posterior cingulum on M^3 is strong and high; and the I_2 is a huge tusk (Ringström, 1924; Qiu and Yan, 1982; Deng, 2001a, 2001c).

The Yinchuan skull also differs from *Acerorhinus* Kretzoi. In *Acerorhinus*, the nasals are long and flat with a smooth tip, and the nasal notch is deep at the level behind the P^4/M^1 boundary; the nasal base is strongly and abruptly constricted, and the ventral surface of the nasals is convex; the lower margin of the zygomatic process on the maxillary is evidently higher than the alveolar border, and the anterior end of the zygomatic arch is not laterally prominent; the braincase is narrow and high, and the occipital surface is forwardly

oblique; the lateral occipital crest is weak, and the lateral margin of the occipital surface has an angular fold at its middle; the mandibular symphysis is strongly uplifted and narrow, with a width smaller the distance between the two P_2s; the horizontal ramus is high; the parastyle fold is well developed, and the lingual cingulum is discontinuous; the protocone is not constricted, and the crochet and bridge are weak or absent on the premolars; the I_2 is a huge tusk with a worn posterior surface; and the metalophid forms an acute angle, and the paralophid is weak or absent (Borissiak, 1914, 1915; Ringström, 1924; Bohlin, 1937; Qiu et al., 1987b; Deng, 2000). On the other hand, *Shansirhinus* and *Acerorhinus* share some important characters, such as a strong facial crest, a strong and straight postglenoid process, and a forwardly inclined ascending ramus of the mandible. As a result, the two genera may be closely related.

The Yinchuan skull differs from *Subchilotherium* Heissig, as well. In *Subchilotherium*, the nasals are moderately long and flat, with a sharp and smooth tip; the nasal base is not constricted, and the ventral surface of the nasals is convex; the lower margin of the zygomatic arch is angularly prominent at its mid-section and the posterior margin is vertical; the braincase is narrow and high; the angle between the basioccipital and basisphenoid bones is large, and the choana is wide; the palate is narrow and flat, and the maxillary tubercle is weak; the mandibular symphysis is narrow and has a shallow sagittal valley; the horizontal ramus is high and has a shallow vasal notch, and the ascending ramus has a large and deep depression on its upper part of the lateral surface; the protocone is not constricted, and the antecrochet is absent; the crista and medifossette are absent, except on M^3, where the medifossette is well developed; the lingual cingulum is discontinuous, and the enamel plications are absent on the premolars; the anterior, posterior, and lingual cingula on the molars are well developed, and the lingual cingulum is a very strong pillar on M^3; the metacone valley is very prominent; the I_2 is a huge tusk; the posterior valley of P_2 is very narrow; and the trigonid is rounded and has an acute metalophid and a weak or absent paralophid (Heissig, 1972; Deng, 2005).

4. Revision

An incomplete right maxillary with P^2-M^1 (V 4316) from Banguo in Yuanmou (Yunnan, China) was described as a new species, *Ch. yunnanensis* (Tang et al., 1974). Comparing the Banguo specimen with *R.* aff. *brancoi* from Huangshigou (Ringström, 1927), the authors stated that the labial wall of *Ch. yunnanensis* is not extended posteriorly, the parastyle is not well developed, the parastyle fold is not prominent, the enamel plications are weaker, the width of the teeth are evidently larger than the length, and the protocone on the premolars is strongly constricted. Toward the base of rhinocerotid teeth, however, the metastyle becomes shorter, the enamel plications are weaker, and the protocone is more constricted. The Banguo teeth are more worn than are the Huangshigou

teeth, because the latter belonged to a young individual with a freshly erupted M^3. On the Banguo specimen, only P^3 retains its parastyle and parastyle fold, whereas the other teeth have lost these elements. In fact, the parastyle and parastyle fold on P^3 of the Banguo specimen (Tang et al., 1974: Pl. 1, Fig. 3) are as strong as or slightly stronger than those of the Huangshigou specimen (Ringström, 1927: Pl. 1, Fig. 3), which is also caused by a greater degree of wear in the former. In regard to the tooth width being larger than the length, this feature is common among rhinocerotids (Table 3). Consequently, *Ch. yunnanensis* is a junior synonym of *S. ringstromi*.

Qiu and Yan (1982) established a new chilothere, *Ch. cornutum*, based on an incomplete skull with no occiput, from Hanjiawa in Yushe (Shanxi, China). Qiu et al. (1987b) revised this species into *Acerorhinus cornutus*. Qiu and Yan (1982) did not discuss the relationship of this species to *S. ringstromi* (= *R.* aff. *brancoi*) or *S. brancoi* (= *R. brancoi*). They indicated that the Hanjiawa skull has some characters that differ from those of other species of *Chilotherium*, such as a strongly concave frontal region, short and wide nasals with a rough tip and parallel lateral margins, a relatively small dP^1 with a much lower occlusal surface than is found on other teeth, a strongly constricted protocone and hypocone, and a well-developed lingual cingulum on the premolars. On the other hand, the teeth from the Hanjiawa specimen (Qiu and Yan, 1982: Text-Fig. 5, Pl. 1, Fig. 2) are similar to those from the Huangshigou specimen (Ringström, 1927: Pl. 1. Fig. 3). Both share a relatively small dP^1, a weak or absent parastyle fold, a strong lingual bridge, a squarely expanded hypocone and well-developed medifossettes on the premolars. In addition to these common dental characters, the Hanjiawa skull is comparable to the Yinchuan skull. Both skulls have the short and uplifted nasals with a small and lunate terminal horn boss, a slightly constricted nasal base, a concave frontal region, a very retracted premaxilla, and a strong and prominent supraorbital tubercle. Conversely, the Hanjiawa skull greatly differs from *Acerorhinus* Kretzoi with the presence of short and uplifted nasals, a slightly constricted nasal base, a flat labial wall of the upper cheek teeth, and a strongly constricted protocone and well-developed lingual bridge on the premolars. As a result, we referred *A. cornutus* into *S. ringstromi*.

Zheng (1982) described another new chilothere, *Ch. tianzhuensis*, based on an incomplete maxillary with P^2-M^2 (V 6416) and some isolated teeth from Songshan in Tianzhu (Gansu, China). He suggested that this species is similar to *Ch. cornutum* Qiu and Yan from Hanjiawa with respect to the strongly molariform premolars, the widened cheek teeth, the strongly constricted protocone, the well-developed crochet and crista forming a medifossette with enamel plications, and the weak parastyle and parastyle fold. He hypothesized that *Ch. tianzhuensis* might be united with *Ch. cornutum* into the same species if the skull of the Tianzhu species is discovered. His hypothesis is reasonable. In fact, the dental characters of the Tianzhu specimens are similar to those of *S. ringstromi*. They share a weak or absent parastyle fold, a well-developed crochet and crista, strong medifossettes with prominent

enamel plications, and a wide lingual bridge on the premolars. Likewise, as with *Ch. cornutum*, *Ch. tianzhuensis* should be revised to be included within *S. ringstromi*.

5. Phylogenetic discussion

Schlosser (1903) suggested that *R. brancoi* was related to both *Rhinoceros habereri* from China and *Aceratherium angustifrons* from Samos. Kretzoi (1942) believed that *Shansirhinus* was a branch of a close lineage of *Chilotherium*, because *Chilotherium* has the characteristic lingual bridge of *Shansirhinus*, but has no enamel plications. He indicated that the cranial structure of *A. angustifrons* was different from that of *Chilotherium*.

The general cranial and dental morphologies of *Chilotherium* are fairly well known (Ringström, 1924; Heissig, 1975; Deng, 2001a, 2001c), and will not be repeated here except for those of phylogenetic relevance to this comparison. Based on the form of the lower incisors, Heissig (1989) considered that *Chilotherium* might have originated from the same group that began in the early Middle Miocene of South Asia with *Subchilotherium* Heissig, from the lower Siwalik series. According to cladistic analyses, Prothero et al. (1986); Geraads and Koufos (1990) suggested that *Chilotherium* was the sister group of *Aceratherium*. Qiu et al. (1987b) noted that *Chilotherium* was more advanced than *Acerorhinus* and was derived from the latter.

Many of the apparent differences between *Shansirhinus* and *Chilotherium* pertain to dental or cranial characters, and reflect the fundamentally divergent trophic adaptation of these genera: *Shansirhinus* tended toward a grazing direction, whereas *Chilotherium* had dental adaptations that were more suitable for browsing. The highly specialized dental modifications, particularly those in *Chilotherium*, leave a thick morphological overprint that obscures the phylogenetic relationship. The following is a list of derived characters shared by *Shansirhinus* and *Chilotherium* that, despite the morphological overprint, suggest a possible sister relationship of the genera. Additionally, the *Shansirhinus–Chilotherium* clade may be the sister group of the genus *Acerorhinus*. Polarity is determined through comparisons with the following outgroups from the basal members of major clades of rhinocerotoids: basal rhinocerotoiform *Hyrachyus*, hyracondontine *Hyracondon*, rhinocerotid *Trigonias*, and diceratherine *Diceratherium*.

Mandibular symphysis—The mandibular symphysis in aceratherines is usually very narrow with a smaller width than the distance between the two P_2s. The laterally expanded symphysis in *Shansirhinus* and *Chilotherium*, especially in the shovel-like anterior part (Fig. 5(2)), is prominent and apparently unique to these two genera among aceratherines.

Ventral surface of mandibular symphysis—The ventral surface of the mandibular symphysis in *Chilotherium* and *Shansirhinus* is deeply concave, as opposed to the more shallowly concave or flat ventral surface present in most basal aceratherines.

Premaxilla—The retraction and relative size of the premaxilla are nearly identical in *Shansirhinus* and *Chilotherium*, as in the lack of the upper incisors forming two flakes. While the chisel-tusk shearing complex of I^1 and I_2 essentially retains the primitive condition for the Rhinocerotidae (Radinsky, 1966), the loss of the upper incisors is certainly a derived character. The fact that *Ceratotherium* and *Diceros* have no upper incisors suggests that those in *Shansirhinus* and *Chilotherium* may be a synapomorphy acquired independently of living rhinocerotids.

Facial crest—The facial crest in *Chilotherium* develops a right angle on the maxillary face. This strong crest appears homologous to the facial crest in *Shansirhinus*, which also forms a right angle (Fig. 3(1)). Although a weak facial crest may exist in some aceratherines that extends upward to form an acute angle on the maxillary face, the formation of a prominent right angle by this crest in *Chilotherium* and *Shansirhinus* represents a unique occurrence in the two genera.

Dorsal skull profile—Both *Chilotherium* and *Shansirhinus* have the primitive condition of a flat or slightly concave dorsal skull profile. Primitively, the dorsal skull profile is very flat, as shown in *Hyrachyus*, *Trigonias*, *Subhyracodon*, and *Diceratherium*.

Parastyle fold—Primitively, the parastyle fold is strong and prominent. In *Shansirhinus*, the parastyle fold is weak or absent (Fig. 6(1)). This weakness or absence of the parastyle fold is extremely developed in *Chilotherium*, as is evidenced by a very flat labial wall of the upper cheek teeth.

Protocone—The protocone in most rhinocerotoids is not constricted. In some aceratherines, the paracone is constricted to form the anterior and posterior protocone grooves. In *Chilotherium*, the strongly constricted protocone produces a robust and long antecrochet. *Shansirhinus*, however, does not have an antecrochet on its premolars, and it has a well-developed lingual bridge.

Based on comparisons with outgroups such as *Hyrachyus*, *Hyracondon*, *Trigonias*, and *Diceratherium*, the following cranial, mandibular and dental features are likely to be morphotypical conditions for a *Shansirhinus–Chilotherium* clade: a strongly retracted premaxilla, an expanded mandibular symphysis with a larger width than the distance between the two P_2s, a weak or absent parastyle fold, a strongly constricted protocone, a deeply concave ventral surface of the mandibular symphysis, a rounded braincase, and a well-developed antecrochet. Regarding the mandible, however, the strongly expanded symphysis in *Chilotherium* is obviously autapomorphous, and the more primitive symphysis morphology in *Shansirhinus* is closer to the primitive condition of the *Shansirhinus–Chilotherium* clade.

6. Biostratigraphy and paleoecology

R. brancoi, described by Schlosser (1903), was collected as "dragon bones" from traditional Chinese drugstores in Shanghai and Tianjin. Therefore, the exact collection locality and age are impossible to determine.

R. aff. *brancoi* was collected from Huangshigou in Yushe (Shanxi, China), and no other mammalian fossils were reported from this locality (Ringström, 1927). Huangshigou is located in the Nihe district in the Yushe Basin, and the Neogene strata are very thick and well exposed in this district. Qiu et al. (1987a) indicated that the mammalian fossils in Nihe have been recovered mainly from the Lower Pliocene Gaozhuang Formation. Therefore, the partial maxillary (M 536) of *S. ringstromi* (= *R.* aff. *brancoi*) may have been collected from the Gaozhuang Formation. The skull of *A. cornutus* was also collected from the Yushe Basin, but at Hanjiawa in the Haobei district, approximately 20 km from Nihe. In Haobei, the mammalian fossils have been recovered from the Late Miocene Mahui Formation with a paleomagnetic age of 5.2–6 Ma, corresponding to the late Turolian Age (MN13) (Qiu et al., 1987a, 1999).

The *Hipparion* fauna from the Linxia Basin is presently correlated with the Chinese Baodean and Gaozhuangian, and corresponds to the European Vallesian to Ruscinian (MN9-15 in Mein, 1999) *Hipparion*-bearing strata (Qiu and Xie, 1998; Deng, 2001b). Within the various localities of the Linxia Basin, four *Hipparion*-bearing assemblages have been recognized: the Guonigou locality bears the oldest fauna, the Dashengou locality bears the second-oldest, the Yangjiashan locality bears the third, and the Shilidun locality bears the youngest fauna. A paleomagnetic section in the Linxia Basin indicates that the *Hipparion*-bearing strata from the red clay are restricted to an interval of 11.42–4.34 Ma (Fang et al., 1997).

The Yinchuan skull was collected from the red clay of the Hewangjia Formation. Other mammalian fossils have been discovered at the same formation at Shilidun, which is in close proximity to Yinchuan in the Linixa Basin. The additional taxa include *Hystrix gansuensis*, *Promephitis* sp., *Chasmaporthetes* sp., *Hyaenictitherium wongii*, Proboscidea, *Hipparion* sp., *Cervavitus novorossiae*, *Palaeotragus* sp., and *Sinotragus* sp., which indicates that the Hewangjia Formation is Early Pliocene in age. Paleomagnetic analyses have dated the red clay of the Hewangjia Formation from 6.16 to 4.34 Ma. Because the Yinchuan skull is found from the upper part of the Hewangjia Formation, its age corresponds to MN15 of the Ruscinian Age.

The Banguo Fauna includes *Ch. yunnanensis* from Yuanmou (Yunnan, China) and other mammalian fossils, such as *Enhydriodon* cf. *falconeri*, Hyaenidae, *Mastodon* sp., *Stegolophodon banguoensis*, *Stegodon primitium*, ?*Hipparion* sp., and *Sus* sp., which indicate an Early Pliocene age (Tang et al., 1974).

In the Songshan Fauna from Tianzhu (Gansu, China), 31 mammalian species coexist with *Ch. tianzhuensis* (Zheng, 1982). This fauna is considered to be Late Miocene in age, corresponding to MN12 of the Turolian Age (Qiu and Qiu, 1995).

In summary, *S. ringstromi* is distributed chronologically from the late Baodean to the Gaozhuangian Ages in the Chinese Neogene, which corresponds to the period from MN12 of the Turolian Age to MN15 of the Ruscinian Age. Among this

species, size follows an increasing trend, and enamel plications strengthen through time. *S. ringstromi* may be the ancestor of the more derived or specialized *S. brancoi*.

Qiu and Yan (1982) discussed the feeding habits of *S. ringstromi* (= *Ch. cornutum*), and considered it to be adapted to browsing leaves and soft twigs. On the other hand, the high crown and the strong wear of the teeth of *Shansirhinus* imply that it grazed tough grasses. The well-developed secondary folds (crochet, antecrochet, crista, medifossette, constricted protocone, and lingual bridge) and enamel plications can more efficiently provide a means for the teeth of *Shansirhinus* to resist the abrasion of high-fiber diets. Thus we conclude that *Shansirhinus* was a grazer because it has a premolar morphology unique to certain rhinoceroses and horses, such as *Elasmotherium* and *Hipparion* that have the grazing adaptations of high-crowned and strong plicate teeth. The dominant mammalian taxa accompanying *Shansirhinus* are rodents, perissodactyls and artiodactyls (Tang et al., 1974; Zheng, 1982), which indicates an open and dry ecological environment.

Acknowledgements

References

Borissiak, A., 1914. [Mammifères fossiles de Sebastopol, I]. Trudy Geolegicheskago Komiteta. Novaja Seria 87, 1–154 [in Russian].

Borissiak, A., 1915. Mammifères fossiles de Sebastopol, II]. Trudy Geolegicheskago Komiteta. Novaja Seria 137, 1–45 [in Russian].

Bohlin, B., 1937. Eine tertiäre Säugetier-Fauna aus Tsaidam. Palaeontologia Sinica C 14, 1–111.

Deng, T., 2000. A new species of *Acerorhinus* (Perissodactyla, Rhinocerotidae) from the Late Miocene in Fugu, Shaanxi, China. Vertebrata Palasiatica 38, 203–217.

Deng, T., 2001a. New materials of *Chilotherium wimani* (Perissodactyla, Rhinocerotidae) from the Late Miocene of Fugu, Shaanxi. Vertebrata Palasiatica 39, 129–138.

Deng, T., 2001b. New remains of *Parelasmotherium* (Perissodactyla, Rhinocerotidae) from the Late Miocene in Dongxiang, Gansu, China. Vertebrata Palasiatica 39, 306–311.

Deng, T., 2001c. Cranial ontogenesis of *Chilotherium wimani* (Perissodactyla, Rhinocerotidae. In: Deng, T., Wang, Y. (Eds.), Proceedings of the Eighth Annual Meeting of the Chinese Society of Vertebrate Paleontology. China Ocean Press, Beijing, pp. 101–112.

Deng, T., 2002a. Limb bones of *Chilotherium wimani* (Perissodactyla, Rhinocerotidae) from the Late Miocene of the Linxia Basin in Gansu, China. Vertebrata Palasiatica 40, 305–316.

Deng, T., 2002b. The earliest known wooly rhino discovered in the Linxia Basin, Gansu Province, China. Geological Bulletin of China 21, 604–608.

Deng, T., 2003. New material of *Hispanotherium matritense* (Rhinocerotidae, Perissodactyla) from Laogou of Hezheng County (Gansu, China), with special reference to the Chinese Middle Miocene elasmotheres. Geobios 36, 141–150.

Deng, T., 2005. Rhinocerotid fossils from the hominoid site in Yuanmou. Yunnan, China. In: Qi, G.Q., Dong, W. (Eds.), *Lufengpithecus hudienensis* Site. Science Press, Beijing (in press).

Fang, X.M., Li, J.J., Zhu, J.J., Chen, H.L., Cao, J.X., 1997. Absolute dating and division of the Cenozoic strata of the Linxia Basin in Gansu. Chinese Science Bulletin 42, 1457–1471 [in Chinese].

Geraads, D., Koufos, G., 1990. Upper Miocene Rhinocerotidae (Mammalia) from Pentaloph-1, Macedonia, Greece. Palaeontographica Abteilung A 210, 151–168.

Guan, J., 1988. The Miocene strata and mammals from Tongxin, Ningxia and Guanghe, Gansu. Memoirs of Beijing Natural History Museum 42, 1–21.

Guan, J., Zhang, X., 1993. The Middle Miocene mammals from Guanghe and Hezheng in northwestern China. Memoirs of Beijing Natural History Museum 53, 237–251.

Guérin, C., 1980. Les rhinocéros (Mammalia, Perissodactyla) du Miocène terminal au Pléistocène supérieur en Europe occidentale: comparaison arec les espèces actuelles. Documents des Laboratoires de Géologie de Lyon 79, 1–1182.

Heissig, K., 1972. Paläontologische und geologische Untersuchungen im Tertiär von Pakistan, 5. Rhinocerotidae (Mamm.) aus den unteren und mittleren Siwalik-Schichten. Bayerische Akademie der Wissenschaften Mathematisch—Naturwissenschaftliche Klasse. Abhandlungen, Neue Folge 152, 1–112.

Heissig, K., 1975. Rhinocerotidae aus dem jungtertiär Anatoliens. Geologisches Jahrbuch. Reihe B 15, 145–151.

Heissig, K., 1989. Rhinocerotidae. In: Prothero, D.R., Schoch, R.M. (Eds.), The Evolution of Perissodactyls. Oxford University Press, New York, pp. 399–417.

Heissig, K., 1999. Family Rhinocerotidae. In: Rössner, G.E., Heissig, K. (Eds.), The Miocene Land Mammals of Europe. Verlag Dr. Friedrich Pfeil, München, pp. 175–188.

Kretzoi, M., 1942. Bemerkungen zum System der nachmiozänen Nashorn-Gattungen. Földtani Közlöny 72, 4–12.

Mein, P., 1999. European Miocene mammal biochronology. In: Rössner, G.E., Heissig, K. (Eds.), The Miocene Land Mammals of Europe. Verlag Dr. Friedrich Pfeil, München, pp. 25–38.

Prothero, D.R., Manning, E., Hanson, C.B., 1986. The phylogeny of the Rhinocerotoidea (Mammalia, Perissodactyla). Zoological Journal of Linnian Society 87, 341–366.

Qiu, Z.X., Huang, W.L., Guo, Z.H., 1987a. The Chinese hipparionine fossils. Palaeontologia Sinica. New Series C 25, 1–250.

Qiu, Z.X., Xie, J.Y., Yan, D.F., 1987b. A new chilothere skull from Hezheng, Gansu, China, with special reference to the Chinese "*Diceratherium*". Scientia Sinica B (5), 545–552 [in Chinese].

Qiu, Z.X., Qiu, Z.D., 1995. Chronological sequence and subdivision of Chinese Neogene mammalian faunas. Palaeogeography, Palaeoclimatology, Palaeoecology 116, 41–70.

Qiu, Z.X., Wang, B.Y., Deng, T., Ni, X.J., Wang, X.M., 2002. Notes on the mammal fauna from the bottom of loess deposits at Longdan, Dongxiang County, Gansu Province. Quaternary Sciences 22, 33–38.

Qiu, Z.X., Wu, W.Y., Qiu, Z.D., 1999. Miocene mammal faunal sequence of China: palaeozoogeography and Eurasian relationship. In: Rössner, G.E., Heissig, K. (Eds.), The Miocene Land Mammals of Europe. Verlag Dr. Friedrich Pfeil, München, pp. 443–455.

Qiu, Z.X., Xie, J.Y., 1998. Notes on *Parelasmotherium* and *Hipparion* fossils from Wangji, Dongxiang, Gansu. Vertebrata Palasiatica 36, 13–23.

Qiu, Z.X., Xie, J.Y., Yan, D.F., 1990. Discovery of some Early Miocene mammalian fossils from Dongxiang, Gansu. Vertebrata Palasiatica 28, 9–24.

Qiu, Z.X., Yan, D.F., 1982. A horned *Chilotherium* skull from Yushe, Shansi. Vertebrata Palasiatica 20, 122–132.

Radinsky, L.B., 1966. The families of Rhinocerotoidea (Mammalia, Perissodactyla). Journal of Mammalogy 47, 631–639.

Ringström, T., 1924. Nashorner der *Hipparion*-fauna Nord-Chinas. Palaeontologia Sinica C 1 (4), 1–159.

Ringström, T., 1927. Über quartäre und jungtertiäre Rhinocerotiden aus China und der Mongolei. Palaeontologia Sinica C 4 (3), 1–21.

Schlosser, M., 1903. Die fossilen Säugethiere Chinas nebst einer Odontographie der recenten Antilopen. Abhandlungen der Königlichen Bayerischen Akademie der Wissenschaften 22, 1–221.

Tang, Y.J., You, Y.Z., Liu, H.Y., Pan, Y.R., 1974. New materials of Pliocene mammals from Banguo Basin of Yuanmou, Yunnan and their stratigraphical significance. Vertebrata Palasiatica 12, 60–67.

Zheng, S.H., 1982. Some Pliocene mammalian fossils from Songshan-2 and -3 (Tianzhu, Gansu) and the Songshan Fauna. Vertebrata Palasiatica 20, 216–227.